# Demonstration of Adaptable Quality Radio System for Broadcasting of Speech

Martin Lima and Fredrik Esp Feyling

***Abstract*—This paper is presenting the design and implementation of a radio communication system for broadcasting of speech, with adaptable data rate. This system is to be seen as a "proof of concept", where the main goal is to demonstrate a radio system with feedback from receiver (RX) to transmitter (TX) such that the transmitted data rate adapts to the state of the radio channel. The data rate is varied by a factor 2 by switching between QPSK and QAM-16 modulation, while bandwidth and transmit power is fixed. The proposed system is implemented with a -40dBc bandwidth of 220.6kHz and a transmit power of -10dBm.**

**The adaptive quality feature is verified and the system changes quality immediately when the detected error rate drops below a predefined threshold. The measured bit error rates are $6.0 \cdot 10^{-2}$and $1.4 \cdot 10^{-4}$for high and low data rates respectively. The total delay from transmitter to receiver is measured to 5ms, making the system well suited the for two-way communication as well as broadcasting.**

## I. Introduction

When designing any radio communication system, trade-offs has to be made between bandwidth, power, system complexity and bit rate. For a given bandwidth and transmit power, the bit rate could be varied by using different modulation schemes. As higher order modulation schemes require higher $\frac{E_b}{N_0}$, choosing optimum modulation scheme would require knowledge about the radio channel in order to maintain low enough BER at the receiver. This knowledge may be obtained by adding complexity in form of a feedback channel from receiver to transmitter. By performing some kind of error detection, the receiver may send information about detected error rates back to the transmitter. This enables the system to adapt the data rate to the state of the radio channel, and thus provide better QoS for given power and bandwidth.

In this paper, we present a radio communication system with this kind of feedback structure. The system is to be seen as a "proof of concept" and the goal is not to propose a complete radio system for commercial use. The adaptable quality is obtained by implementing a feedback path from the receiver to the transmitter, using frequency-division duplexing (FDD). In this demonstration we simulate the varying state of the radio channel by changing the transmit power, for a more controllable and reproducible test environment.

Figure 1 shows a top level block diagram of the proposed system. The figure shows that speech data is sent in the forward path from transmitter to receiver, and the number of detected errors is sent in the feedback path from receiver to transmitter. The forward and feedback paths will be referred to as the *data path* and the *BER path* respectively. .

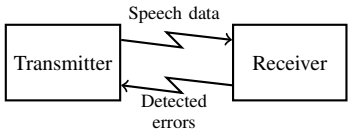


Fig. 1. Top level block diagram of proposed system. Speech data is sent in the forward path from transmitter to receiver and the number of detected errors is sent back from receiver to transmitter.

The proposed system is designed to switch between two different data rates, using two different modulation formats. Figure 2 shows a qualitative illustration of the adaptive quality concept. The proposed system may be further improved by adding more levels, yielding even better utilization of available resources.

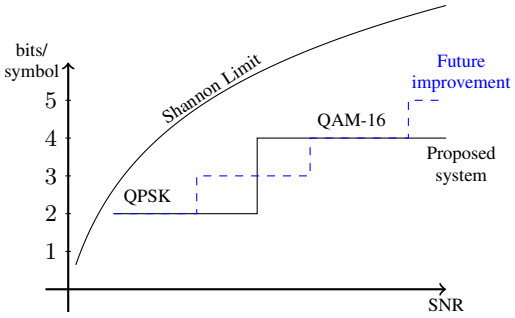


Fig. 2. Qualitative illustration of the adaptive quality concept

Throughout this paper, we will use the word *transmitter* when referring to the radio module that is transmitting the speech data and *receiver* when referring to the module that is receiving it. This is not to be confused with the terms TX and RX, which we use when referring to the transmit and receive port on each radio module.

The system is implemented using the software defined radio USRP-2901 [1] from National Instruments, which contains all necessary RF hardware. All the software parts of the system is implementing in C++ and is executed on a standard personal computer. Pre-written C-libraries are used for the parts of the system concerning interface to the USRP, the computer sound card etc. These parts will not be explained in detail, but references to the libraries will be given. For the remaining parts of the system, we focus on explaining the implementation on a behavioural level and detailed descriptions of C code implementations is avoided.

In section II we present the system specifications and the link budget is presented in section III together with associated measurements. A detailed description of the proposed system is given in section IV and the motivation behind some crucial design decisions is presented in section V. Performed measurements is presented in section VI before a final conclusion is given in section VII.

## II. System Specifications

The proposed radio communication system is designed to switch between QPSK and QAM-16 modulation in order to obtain adaptable sound quality. The system use the 2.4GHz ISM band with a carrier frequency of 2.415GHz and 2.455GHz for the data path and BER path respectively. The system is designed for a transmission distance of 5 meter in an indoor environment.

Some key system specifications are listed in table I and II. Table I shows the parameters for the data path, for low / high data rate transmission. Table II shows parameters for the simpler BER path.

The burst format for the transmitted data is shown in figure 3. The bursts are different when using QPSK and QAM-16 modulation, because the same number of training symbols maps to a different number of bits. The data packets (a and b) is transmitted continuously

TABLE I
SYSTEM SPECIFICATIONS - DATA PATH

| System Variables | Value Low / High Data rate |
|---|---|
| Frequency $f_0$ | 2415 MHz |
| Modulation | QPSK/QAM-16 |
| Sound sampling rate $f_s$ | 11025/22050 Hz |
| Bits per sound sample $b_s$ | 12 bits |
| Sound datarate $R_{ss}$ | 132/265 kbits/s |
| Channel coding | Hamming (4,7) |
| **Packet Parameters** | |
| Packet header size | 8 bits |
| Packet size | 512 bits |
| **Frame Parameters** | |
| Training sequence type | Barker |
| Training sequence length | 26 symbols |
| **Burst Parameters** | |
| Guard period | 2 symbols |
| Burst Length | 484/256 symbols |
| **Transmission Characteristics** | |
| Symbol rate $R_s$ | 150 ksymbols/s |
| Samples per Symbol | 8 |
| Pulse shaping filter | root raised cosine |
| Pulse shaping filter parameter $\alpha$ | 0.5 |
| Minimum Nyquist bandwidth $\Delta f$ | 112, 5 kHz |

TABLE II
SYSTEM SPECIFICATIONS - BER PATH

| System Variables | Value Low / High Data rate |
|---|---|
| Frequency $f_0$ | 2455 MHz |
| Modulation | QPSK |
| Channel coding | Hamming (4,7) |
| **Packet Parameters** | |
| Packet header size | 8 bits |
| Packet size | 26 bits |
| **Frame Parameters** | |
| Training sequence type | Barker |
| Training sequence length | 26 symbols |
| **Burst Parameters** | |
| Burst Length | 43 symbols |
| **Transmission Characteristics** | |
| Symbol rate $R_s$ | 150 ksymbols/s |
| Samples per Symbol | 8 |
| Pulse shaping filter | root raised cosine |
| Pulse shaping filter parameter $\alpha$ | 0.5 |
| Minimum Nyquist bandwidth $\Delta f$ | 112, 5 kHz |

with the indicated guard period. The BER packets is very small compared to the data packets, and is only transmitted ones per received data packet. Thus no guard period is specified for these packets.

Note that this system is implemented with constant payload size, which means that the packet rate is varied when the data rate changes.

## III. LINK BUDGET

The link budget for the system is shown in table III. The system is designed to operate indoors with a distance of 5 meters between transmitter and receiver. Table III shows losses from propagation, loss in TX and RX and some estimated key parameters at the receiver.

In this demonstration, the transmit power is varied in order to simulate changes in the radio channel, while the physical radio link is fixed. Hence no fading statistics is included in the link budget. The stated values are based on the transmit power used for high data rate transmission, corresponding to the best simulated state of the radio channel.

The value for connector loss is taken from the data sheet of a standard coaxial RF connector [2]. The antenna gain value is taken

| Training sequence 52 | Session ID 3 | Packet ID 5 | Payload 512 | Guard bits 4 |
|---|---|---|---|---|

(a) QPSK data packet

| Training sequence 104 | Session ID 3 | Packet ID 5 | Payload 512 | Guard bits 8 |
|---|---|---|---|---|

(b) QAM-16 data packet

| Training sequence 52 | Session ID 3 | Packet ID 5 | Payload 26 |
|---|---|---|---|

(c) QPSK BER packet

Fig. 3. Burst format (bits) for QPSK(a) and QAM-16(b) modulated data packets, and QPSK modulated BER packet (c)

TABLE III
LINK BUDGET

| TX Loss | Value Low / High Data rate |
|---|---|
| PA Power, $P_{PA}$ | $-10$dBm |
| TX Connector Loss, $L_{ConT}$ | $-0.3$dB |
| TX Power, $P_T$ | $-10.6$dBm |
| TX Antenna Gain, $G_T$ | 1.5dBi |
| Effective (Isotropic) Radiated Power, EIRP | $-9.1$dBm |
| **Path Loss** | |
| Distance, $d$ | 5m |
| Floor loss factor, $Pf(n)$ | 0dB |
| Distance power loss coefficient, $N$ | 38 |
| Total ITU path loss, $L_P$ | $-66.22$dB |
| **RX Loss** | |
| RX antenna gain, $G_R$ | 1.5dBi |
| RX connector loss, $L_{ConR}$ | $-0.3$dB |
| Total RX Loss, $L_R$ | 0.9dB |
| **RX Loss** | |
| Total Received Power, $P_R$ | $-74.42$dBm |
| Antenna Noise Density, $N_0$ | $-145.73$dbm/Hz |
| Antenna Total Noise Power, $N$ | $-92.72$dBm |
| RX Noise Figure, $NF$ | 7.0dB |
| **RX Properties** | |
| Carrier-to-noise ratio, $C/N$ | 11.3dB |
| Eb over N0, $E_b/N_0$ | 9.54dB/6.23dB |

from the data sheet [3].The transmit power, $P_{PA}$, was adjusted after measurements to obtain appropriate $E_b/N_0$ at the receiver.

The estimated path loss constitutes solely of the propagation loss obtained from the ITU Indoor Propagations Loss Model [4]. The loss model consists of two adjustable factors, the distance power loss coefficient, $N$, and the floor loss penetration factor, $P_f(n)$. The latter is set to 0, and the former was set to 38 after calibrating the test environment. Figure 4 shows the measured path loss and the prediction from the ITU model before and after adjusting the power loss coefficient.

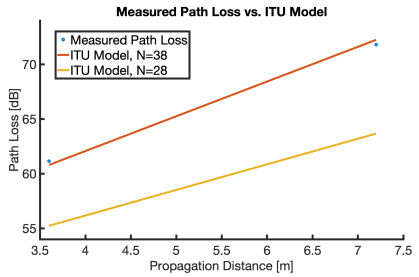


Fig. 4. Measured path loss vs. estimated path loss from the ITU Indoor Propagations Loss Model, before and after adjusting the power loss coefficient

Other loss factors such as pointing loss and polarisation loss was

considered, but measurements showed that the amount of reflections in the room made pointing and polarisation irrelevant to the received power.

The antenna noise density was measured with a spectrum analyser and the estimated value was taken as an average of several single runs. The noise figure of the receiver is included to account for noise added by the radio hardware, with value taken from the data sheet.

## IV. Design Description

Figure 1 shows how the transmitter and receiver communicates within the system. Block diagrams for the two subsystems are shown in appendix A, figure 13 and 14. The data rate between each block of the data path is indicated with the thin arrows. The behaviour of the system will be explained in this section.

Because two different modulation schemes are used, the receiver need to know how to decode the incoming data packets. This problem is solved by using two different training sequences in the beginning of each frame. As shown in figure 13, after frame sync, the receiver perform a check on the received Barker sequence before de-mapping the symbols.

In the transmitter, a variable called *Session State* keep the information about what data quality and modulation scheme to use. As figure 13 indicates, the session state influences several blocks of the TX side of the transmitter. The decision of when to change data quality is left completely to the transmitter. For every received data packet, the receiver computes the number of detected errors and transmit this number back to the transmitter. These BER packets are always transmitted using QPSK-modulation. Based on the received number of detected errors the transmitter decides whether to change session state or not.

The sound producer and sound consumer contains functionality for handling the sound input and output to the sound card of the computer. They are implemented using the Windows API [5]. Sound producer reads sound samples from the sound card at full quality (16 bit, 44100 Hz stereo) and writes the samples to a queue accessible for the source encoder. Sound consumer equivalently reads sound samples from a queue controlled by the unpacking block and writes to the computer sound card.

The source encoder performs lossy compression of the produced sound samples. The bit resolution is reduced to 12 bit per sound sample, and the sampling rate is reduced by a factor 2 or 4 depending on the session state. The source decoder performs the inverse operation, writing 2 or 4 copies of the same sample to the sound consumer.

In the packing block, sound data is read from the source encoder, a header is added, and the packet is sent to the packet queue. The eight bit packet header consist of a three bit session ID and a five bit packet ID.

A scrambler is implemented before FEC, which computes a bitwise XOR between a pseudo random bit string and the packet. The bit string used for scrambling is of the same size as the packet itself. The scrambler performs the exact same operation at RX and TX.

The implemented FEC algorithm is Hamming (7,4). The implementation is a fast, pre-written C-code, written by Michael Dipperstein [6].

The system uses Grey Code for mapping the binary data to a complex vector $z$. The mapping schemes are shown in figure 5.

The training sequence is added to both I and Q symbols in the block *Add Barker*. The training sequence is an appropriate repetition of Barker sequences of length 7 and 13 for QPSK and QAM-16 modulation respectively. The total length of the training sequence is 26 symbols.

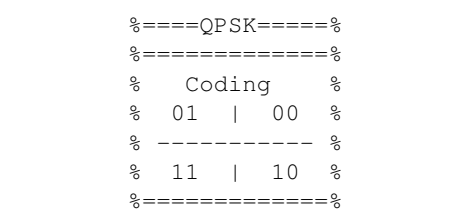


(a)

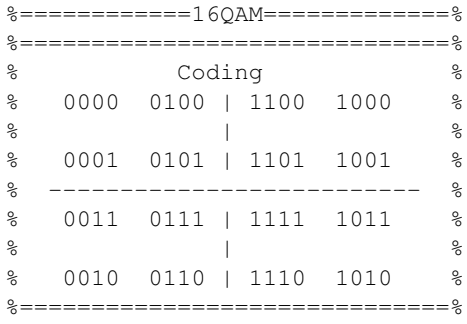


(b)

Fig. 5. Symbol mapping for QPSK (a) and QAM-16 (b) modulated symbols

In the last step before transmission, the symbols are upsampled by a factor $8$ and filtered with a pulse shaping filter. The filter is Root Raised Cosine with a roll-off factor of 0.3. The same filter is applied as a matched filter in the first step at the receive side before the samples are downsampled again.

The USRP is configured to transmit continuously with a symbol rate of $150$ symbols per second and transmit arrays of zeros when no data is available. The USRP interface is implemented using the NI-USRP DLL [7].

Symbol synchronisation is done by choosing the sample offset that maximizes the signal energy.

Frame synchronisation is done by computing the crosscorrelation between the two training sequences and the received symbols. The value of the crosscorrelation is compared to a pre set threshold. The first index that gives a value exceeding this threshold is considered to be the beginning of the frame. After a frame is found, only the frame symbols are passed along to the next block.

### A. Frequency and Phase Synchronisation

The implemented frequency synchronisation algorithm is based on the Mth-power algorithm [8], which is further improved by using a Kalman filter. Frequency offset is estimated from the training sequence only. The Mth-power algorithm estimates the phase offset of MPSK modulated symbols, by mapping all symbols to the same point in the complex plane. By tracking the angular difference between consecutive symbols, the frequency offset may be estimated. In our case, the QPSK symbols of the training sequence is raised to the 4th power, and the phase is estimated as indicated in figure 6.

For each received frame, the frequency offset is estimated by the mean of the angular difference between all consecutive symbols of the training sequence. The estimate obtained from a single frame at time $k$ is referred to as $\widetilde{\omega}_k$.

The accuracy of the estimate is improved by using a Kalman filter. The state of the Kalman filter is the one-dimensional state vector $\omega_k$ which is the true frequency offset between the transmitter and the receiver at time $k$ (i.e. frame $k$). The state is represented by the *a posteriori* state and variance estimate $\widehat{\omega}_{k|k}$ and $\widehat{\sigma}_{k|k}$, where the

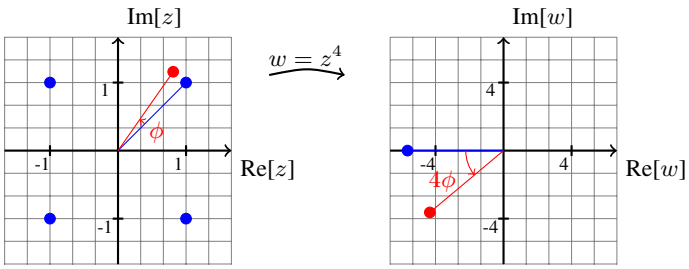


Fig. 6. Illustration the mapping $w = z^4$ which indicates how a phase error in QPSK modulated signal can be observed.

subscript $n|m$ indicates the estimate of time $n$ given observations up to and including time $m \leq n$.

The estimate is obtained in two stages, referred to as the *prediction stage* and the *update stage*. In the prediction stage, the *a priori* estimates $\widehat{\omega}_{k|k-1}$ and $\widehat{\sigma}_{k|k-1}$ is obtained by equations 1 and 2. $\sigma_f$ is the stationary variance of the process noise and must be tuned carefully in order to obtain appropriate convergence speed. In our system $\sigma_f$ was set to $0.8 \cdot 10^{-6}$.

$$\widehat{\omega}_{k|k-1} = \widehat{\omega}_{k-1|k-1} \tag{1}$$

$$\widehat{\sigma}_{k|k-1} = \widehat{\sigma}_{k-1|k-1} + \sigma_f \tag{2}$$

In the update stage, the *a posteriori* estimates $\widehat{\omega}_{k|k}$ and $\widehat{\sigma}_{k|k}$ is obtained by equations 3 and 4. $\widetilde{\omega}_k$ and $\widetilde{\sigma}_k$ is the observed frequency offset and estimated observation noise at time $k$ respectively.

$$\widehat{\omega}_{k|k} = \widehat{\omega}_{k|k-1} + \frac{\widehat{\sigma}_{k|k-1}}{\widehat{\sigma}_{k|k-1} + \widetilde{\sigma}_k}(\widetilde{\omega}_k - \widehat{\omega}_{k|k-1}) \tag{3}$$

$$\widehat{\sigma}_{k|k} = \widehat{\sigma}_{k|k-1}\frac{\widetilde{\sigma}_k}{\widetilde{\sigma}_k + \widehat{\sigma}_{k|k-1}} \tag{4}$$

After the estimates $\widehat{\omega}_{k|k}$ and $\widehat{\sigma}_{k|k}$ is obtained, $\widehat{\omega}_{k|k}$ is applied to each symbol in frame $k$. The phase offset is then estimated as the mean of the angular deviation between the training sequence of the received symbols, and the ideal Barker sequence.

## V. Design Motivation

The goal of the proposed system is to demonstrate a radio communication system with adaptable sound quality. This main goal is the background for all design choices that is made. In this section, the motivation behind the key specifications and some of the solutions described in section IV is given.

### A. System specifications

*1) Transmit Power:* As shown in table III, the transmitter PA power, $P_{PA}$, is set to -10dBm. As the purpose of the system is to demonstrate the adaptable quality feature, the transmit power was tuned to a value suitable for this purpose. Too high transmit power would give a received $E_b/N_0$ high enough to always transmit at the best quality, thus disabling us from demonstrating the quality adoption.

*2) Modulation Scheme:* The system uses QPSK for low data rate transmission and QAM-16 for high data rate transmission. QPSK has the advantage of constant symbol amplitude and therefore reduces nonlinear effects in the amplifiers. Because of the orthogonality between the I and Q signals, QPSK also gives twice the capacity as BPSK for same $E_b/N_0$ sensitivity. QAM-16 is chosen for high data rates because the information content in each symbol is twice as big as for QPSK, making the difference big enough to demonstrate an audible effect.

*3) Bandwidth:* The motivation behind the adaptable quality feature, is to maximise data rate, for fixed bandwidth and transmit power. To demonstrate this feature, the system is designed width a fixed bandwidth, equal for both quality levels. The specific value for the bandwidth is however not important for this demonstration. The transmitted symbol rate is chosen large enough to enable both QPSK and QAM-16 transmission. The ideal Nyquist bandwidth is calculated from the symbol rate and the properties of the pulse shaping filter, and presented in table III.

### B. System Architecture

The adaptable quality feature requires some additional logic, compared to a system without a feedback path. One important design choice is to determine where the decision of changing quality level (referred to as *state*) is to be made. During the design of the proposed system, two solutions were considered:

1) The receiver decides when to change state and sends a simple message to the transmitter, telling it to change state. The receiver has its own state variable, and updates it after sending the message to the transmitter.
   The advantage of this solution is that the receiver always know how the received symbols are modulated. Thus, no state information is needed in the transmitted packet.
   The draw back is that there will be some delay from the receiver ask for a change of state, until state change is completed. This will either cause a few packets to get lost in the meantime, or extra logic must be implemented to handle the issue. Extra logic must also be implemented to handle the case of bit errors in the "change-state-message".
2) The transmitter decides when to change state and the receiver continuously send information about detected error rate to the transmitter. This requires information about the state to be contained in the data packet and the receiver will need more complexity in order to determine the incoming modulation format. However, this will eliminate the senario when the transmitter and the receiver are in different states.

We chose to implement the second solution. The state information is kept in the two different Barker sequences. Because we would have to search for one Barker sequence in the frame synchronisation anyway, searching for one more would be both computationally fast and easy to implement. In addition, the good autocorrelation properties of the Barker sequence makes the state information robust against noise, and no extra FEC is needed to keep this information safe.

### C. Implemented Functionality

*1) Source Enconding:* We chose not to implement any source encoding except for the primitive reduction of data rate. A source encoder removes redundancy in the speech data and increase the information content of every transmitted symbol. This functionality is not necessary to demonstrate the adaptable quality and is therefore not implemented.

The source encoder also makes the system more sensitive to bit errors, as the information content in each bit is increased. Our system is designed to operate at $E_b/N_0$ low enough to demonstrate the quality adaption. When the received $E_b/N_0$ falls low enough to make the system change from QAM-16 to QPSK modulation, we would like the system to have a large margin before the BER for QPSK also get too high and the link is broken. Using a source encoder would make this window smaller and the system would be harder to demonstrate.

*2) Scrambler:* Analysis of the received constellation diagram clearly showed that some symbols occurred more frequently at the receiver than others. Both the RF hardware and the pulse align algorithm are highly sensitive unequal energy distribution between I and Q. When comparing the received constellation from speech data to the constellation from random data, we could see that the quality was considerably increased when transmitting white data. We therefore implemented a scrambler to whiten the speech data before transmission.

*3) FEC:* The implemented FEC algorithm is Hamming(7,4) and serves two purposes. In the data path, the receiver must estimate the number of bit errors and send this number back to the transmitter. In the BER path, the transmitter use the FEC to determine if the received BER packet is valid or not. If the number of bit errors in the BER packet is above a predefined threshold, the packet is considered as invalid in order to reduce the risk of undesired changes of quality level.

This particular algorithm was chosen for its simplicity and decent trade-off between redundancy overhead and minimal Hamming distance. The algorithm allows for detection of any two-bit errors in every 7 bit code word, which was considered sufficient for this purpose. In addition, pre-written C-code implementation exists [6] which saved development time. More advanced FEC algorithms should be considered for applications where bandwidth limitations require less overhead, or error correction is necessary.

*4) Frequency and Phase Synchronisation:* The Mth-power algorithm is chosen for frequency synchronisation because of the good accuracy and simple implementation. By estimating the frequency offset as the mean of the angular deviation between all consecutive symbols, the ML estimate of the frequency offset is obtained. In addition, the Mth-power algorithm does not require a known training sequence, and may be applied to all data samples when QPSK modulation is being used. By extending the algorithm to a Kalman filter, the mean square error between the estimated offset and the actual offset is minimized. The improvement from the Kalman filter is clearly seen in figure 7 which shows the estimated frequency offset at the receiver with and without Kalman filter.

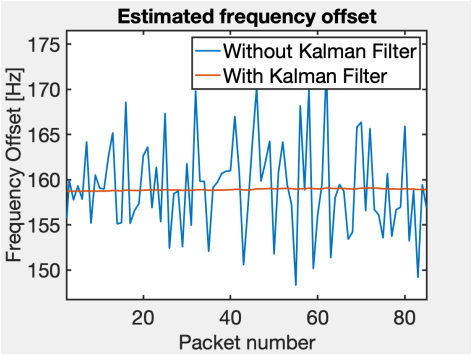


Fig. 7. Estimated frequency offset with and without Kalman filter

The Mth-power algorithm is however not linear, making it less suited for phase estimation. Therefore, the linear algorithm based on comparing the phase directly to the training sequence is used for estimating the phase.

## VI. Measurements and Verification

In this section we present measurements and verifications of the proposed system. We first present a verification of the system specifications in section VI-A. In section VI-B the system performance will be evaluated under different conditions, and some key performance parameters will be presented.

### A. Verification of System Parameters

The verified system specifications is summarised in table IV.

TABLE IV
Summarised Measurements of System Parameters

| System Parameter | Measured Value |
|---|---|
| Half-Power Bandwidth | 220.6kHz |
| PA power, $P_{PA}$ | $-10$dBm |
| Delay | 5ms |

The power spectrum of the signal was analyzed in MATLAB's signal analyzer toolbox [9]. The baseband power spectrum is shown in figure 8 together with the theoretical spectrum. The -40dBc bandwidth is measured to 220.6kHz. The transmit power was verified by first calibrating the USRP power spectral density using a spectrum analyser, and then calculating the total transmit power from measured bandwidth[1]. This way, the transmit power was measured to $-10$dBm.

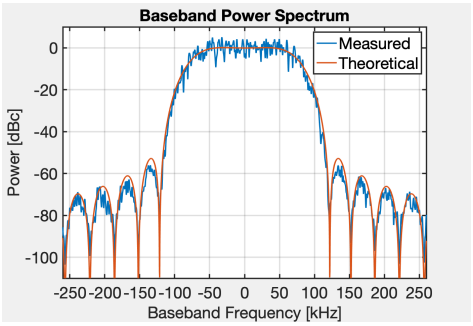


Fig. 8. Received signal power spectrum

The system delay was measured by transmitting a known bit sequence and evaluating the time delay from sound producer to sound consumer. The delay was measured by running both the transmitter and receiver software on the same computer. The average measured delay was 5ms with a sample standard deviation of 2ms.

### B. Performance Measurements

The system is tested in an indoor environment with both USRP's at the same height, 1 meter apart and no polarization mismatch[2]. For the sake of reproducibility, we chose to simulate the varying state of the radio channel by adjusting the transmit power instead of changing the radio channel physically. Two different transmit power levels was used to verify transmission at both qualities. High quality transmission was measured with a transmit power of $-10$dBm and low quality with $-25$dBm.

Eye diagram and constellation diagram is provided for both transmit power levels and both modulation formats, together with some key performance measurements. The diagrams for high and low transmit power are summarised in figure 9 and 10 respectively. Estimated performance parameters are summarised in table V and VI for high and low transmit power respectively. In the tables, BER is the true measured bit error rate and error vector magnitude (EVM) and SNR is estimated from the constellation diagrams. EVM is the average magnitude of the error vector normalized to the peak constellation power.

Figure 11 shows the measured BER as a function of estimated $E_b/N_0$. This value is compared to a theoretical BER (Estimated BER)

[1]Due to the CIVID-19 situation the lab equipment was not available for measurements on the implemented system

[2]The measurements had to be performed in a tiny student apartment because the lab was closed

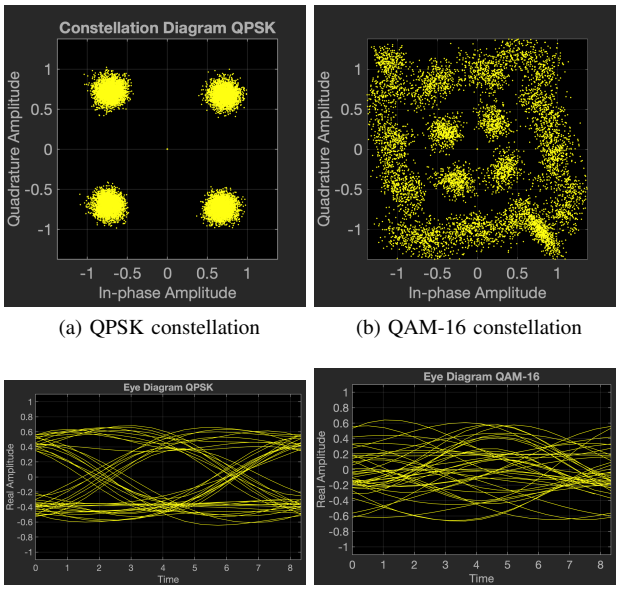


(a) QPSK constellation (b) QAM-16 constellation

(c) QPSK eye diagram (d) QAM-16 eye diagram

Fig. 9. Eye diagram and constellation for QPSK (a and c) and QAM-16 (b and d) modulated symbols. Transmit power: $-10$dBm

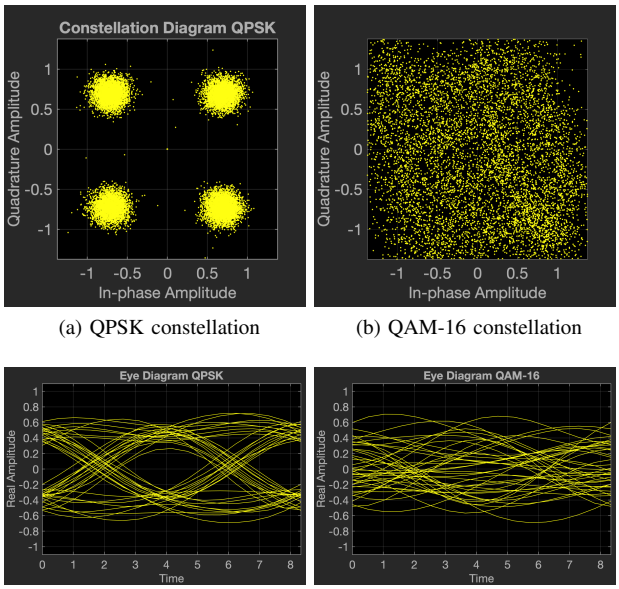


(a) QPSK constellation (b) QAM-16 constellation

(c) QPSK eye diagram (d) QAM-16 eye diagram

Fig. 10. Eye diagram and constellation for QPSK (a and c) and QAM-16 (b and d) modulated symbols. Transmit power: $-25$dBm

TABLE V
MEASURED PERFORMANCE PARAMETERS. TRANSMIT POWER: $-10$dBm

| System Parameter | Measured Value Modulation QPSK / QAM-16 |
|---|---|
| SNR | 18.1dB/12.8dB |
| $E_b/N_0$ | 13.1dB/4.6dB |
| BER | $1.35 \cdot 10^{-5}$/ $6.0 \cdot 10^{-2}$ |
| EVM | $-17.5$dB/ $-14.5$dB |

TABLE VI
MEASURED PERFORMANCE PARAMETERS. TRANSMIT POWER: $-25$dBm

| System Parameter | Measured Value Modulation QPSK / QAM-16 |
|---|---|
| SNR | 15.9dB/10.16dB |
| $E_b/N_0$ | 11.9dB/3.8dB |
| BER | $1.4 \cdot 10^{-4}$/ $1.32 \cdot 10^{-1}$ |
| EVM | $-16.1$dB/ $-12.8$dB |

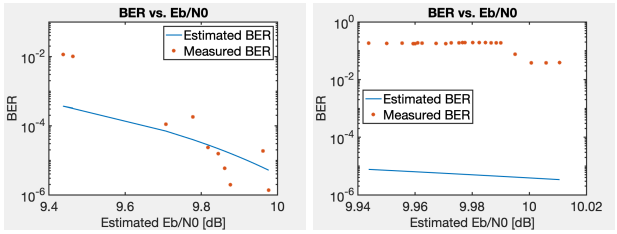


(a) QPSK (b) QAM-16

Fig. 11. BER vs. SNR for both modulation formats. The estimated BER is the theoretical BER based on the estimated values for $E_b/N_0$and true BER is the actual calculated BER

to give an impression of the system performance under the given conditions.

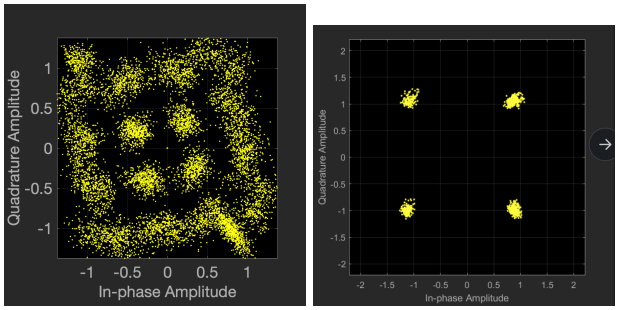


(a) Full frame (b) Barker only

Fig. 12. QAM-16 constellation with full frame and Barker symbols only. Transmit power: $-10$dBm

### C. Discussion of Obtained Results

The proposed system is supposed to broadcast speech data with adaptable sound quality, by switching between QPSK and QAM-16 modulation based on the detected error rates. During the full system test, the threshold for changing state was set to $1 \cdot 10^{-2}$. With this threshold, the system changed quality state when the transmit power was reduced to about $-17$ dBm. The test verified that the adaptable quality feature works as expected. The measured 5ms delay show that the system is well suited for two-way communication as well as broadcasting.

Figure 8 shows that the measured power spectrum lies very close to the theoretical spectrum. This indicates that the amount of nonlinear distortion introduced by the RF hardware is at a minimum.

When transmitting QPSK modulated data at low data rate, the system delivered almost noise free sound, at both power levels. The sound quality was not audibly reduced by the transmission. Figure 9 and 10 and table V and VI supports this qualitative description.

The transmission of QAM-16 modulated data was not equally successful. At the highest power level, the transmitted speech was barely audible. At the lowest power level the sound was completely lost in noise. This result is again supported by figure 9 and 10 and

table V and VI. The constellation diagram in figure 9 (b) shows that the poor quality is mainly due to bad phase synchronization. Figure 12 shows a comparison of the QAM-16 constellation with all frame symbols (a), and with the Barker symbols only (b). As the figure shows, the Barker symbols have no visible phase shift, which indicates that there is a phase difference between the Barker symbols and the rest of the frame. The reason for this problem is not understood by the authors and the issue remains for future improvements.

Figure 11 shows

The plots of figure 11 show that the true BER lies very close to the theoretical BER for QPSK modulation. For QAM-16 however, the true BER is considerably higher than estimated theoretical BER for the given $E_b/N_0$, especially for high $E_b/N_0$values. This is a reasonable result, considering the phase error of this constellation. For high values of $E_b/N_0$, the BER is dominated by phase error causing a gap between theory and measurements. This gap gets smaller as the BER get domi

## VII. Conclusion

The design and implementation of a radio communication system for broadcasting of speech with adaptable data rate is presented. The system adapts the transmitted data rate to the state of the radio channel by evaluating detected bit error at the receiver. The transmitted data rate is varied by a factor 2 by switching modulation format between QPSK and QAM-16.

The system was verified in an indoor environment with a transmission distance of 1 meter and variations in the radio channel is simulated by adjusting the transmit power. The system transmit at high data rate ($520,8$ kb/s) when using QAM-16 modulated symbols at $-10$ dBm and low data rate ($249$ kb/s) for QPSK at $-25$ dBm. Bit error rates of $6.0 \cdot 10^{-2}$and $1.4 \cdot 10^{-4}$was measured at high and low data rate respectively.

The high BER for QAM-16 modulation makes the effect of adaptable quality hardly audible, because of the high noise level when transmitting at high data rate. The adaptable quality feature is however interesting in itself and this demonstration shows a working "proof of concept". By adapting the transmitted data rate to the state of the radio channel, the system yields a better utilization of available resources. This two-level adaption could be extended to several levels for higher performance in future improvements.

## References


[1] National Instruments, "Usrp-2901 specifications - national instruments," https://www.ni.com/pdf/manuals/374925c.pdf, (Accessed on 04/16/2020).

[2] TE Connectivity, "Rf coaxial connectors," https://www.mouser.com/datasheet/2/418/NG_DS_1-1773725-8_RF_COAX_QRG_0114_TE-1948_RFcoaxi-1232379.pdf, (Accessed on 04/14/2020).

[3] Siretta, "Delta-7a datasheet," https://docs.rs-online.com/a8a8/0900766b81540fe9.pdf, (Accessed on 04/14/2020).

[4] International Telecommunication Union, "Recommendation itu-r p.1238-10," https://www.itu.int/dms_pubrec/itu-r/rec/p/R-REC-P.1238-10-201908-I!!PDF-E.pdf, (Accessed on 04/14/2020).

[5] Microsoft Corporation, "Windows api index," https://docs.microsoft.com/en-us/windows/win32/apiindex/api-index-portal, (Accessed on 05/03/2020).

[6] M. Dipperstein, "Hamming (7,4) code discussion and implementation," http://michael.dipperstein.com/hamming/, (Accessed on 04/20/2020).

[7] National Instruments Corporation, "Labview nxg - national instruments," https://www.ni.com/en-no/shop/labview/labview-nxg.html, (Accessed on 05/03/2020).

[8] A. Viterbi, "Nonlinear estimation of psk-modulated carrier phase with application to burst digital transmission," *IEEE Transactions on Information Theory*, vol. 29, no. 4, pp. 543–551, 1983.

[9] MathWorks, "Using signal analyzer app - matlab," https://se.mathworks.com/help/signal/ug/using-signal-analyzer-app.html, (Accessed on 05/02/2020).


## Appendix A
## Block Diagram

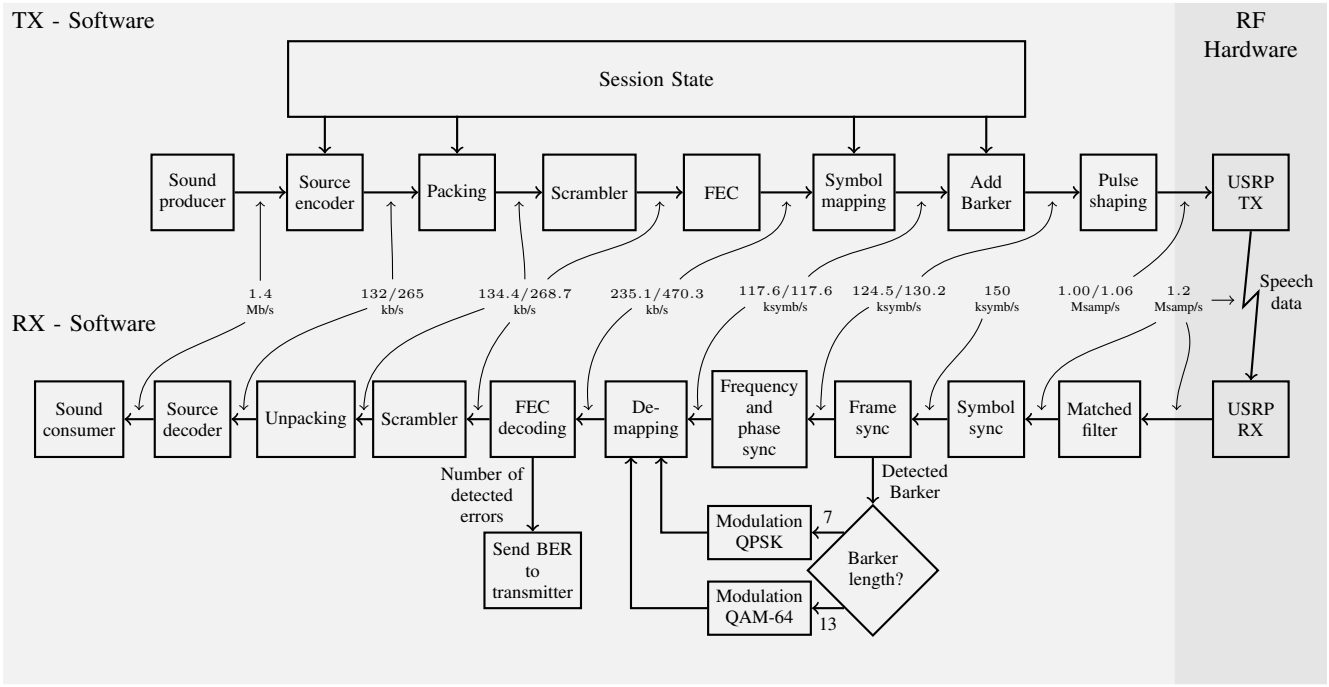


Fig. 13. Block diagram of data packet system. This block diagram shows the forward path of the system, where speech data is being transmitted. Data rates for Low/High data quality is indicated on each arrow.

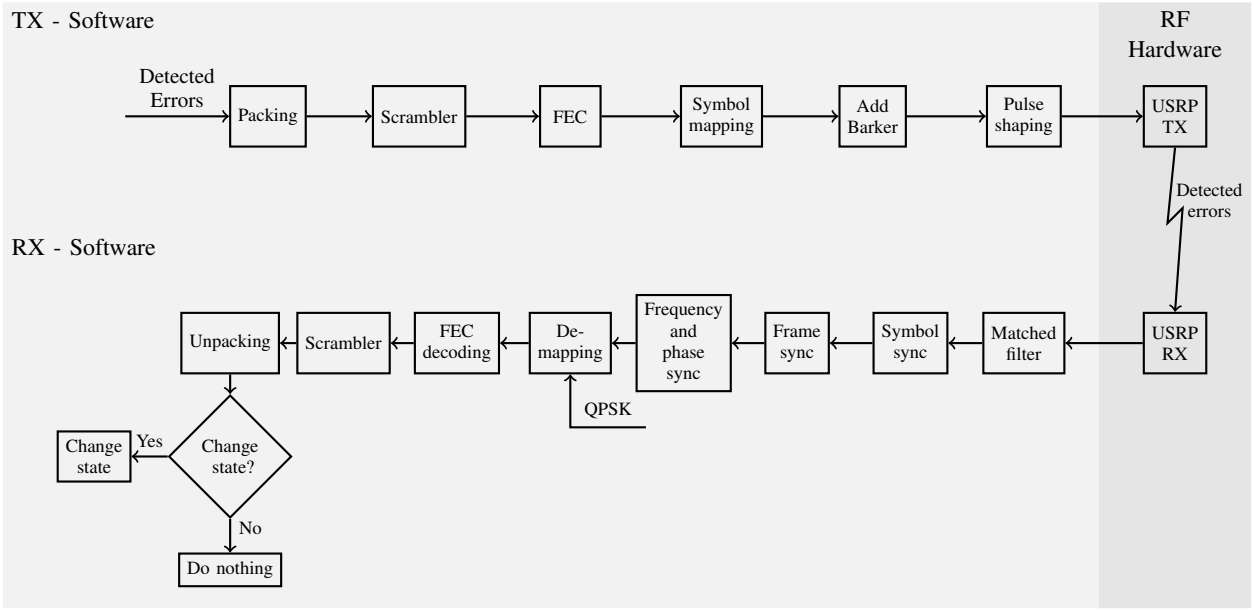


Fig. 14. Block diagram of BER packet system. This sub-system constitutes the feedback path where the receiver transmit information about detected error rate back to the transmitter.